Ecological Indicators 150 (2023) 110257

Contents lists available at ScienceDirect

Ecological Indicators

journal homepage: www.elsevier.com/locate/ecolind

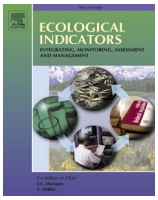

# Projection of future long-term *Aurelia coerulea* biomass variability by regional moderate-temperature-duration approach in the Bohai and Yellow Seas

Yifan Lan, Cuicui Zhang *, Hao Wei

*School of Marine Science and Technology, Tianjin University, Tianjin 300072, China*

ARTICLE INFO

*Keywords:*
Global warming
*Aurelia coerulea* blooms
The Bohai and Yellow Seas
Biomass projection
Regime shifts

ABSTRACT

As temperature is regarded as a significant environmental factor affecting the intensity and frequency of jellyfish blooms, the projection of jellyfish peak biomass variation under global warming becomes essential for disaster prevention and mitigation on long-term time scales. The jellyfish *Aurelia coerulea* is distributed in worldwide oceans, particularly in the Bohai and Yellow Seas (BYSs), which are productive regions with substantial economic and climatic significance and have been suffered from *A. coerulea* blooms. Based on the theory of how *A. coerulea* reacts to various experimental temperature circumstances, recent studies have been proposed to determine the qualitative trends of *A. coerulea* blooms in response to climate change. However, the quantitative study of future *A. coerulea* biomass variability is a challenging task due to the uncertainty in the numerical relation between temperature and the biomasses of *A. coerulea* and the difficulty in determining the biomass considering the high mobility of jellyfishes. In this paper, we develop a moderate-temperature-duration approach to solve these two problems. The temperature suitability for all key life stages of *A. coerulea* during pelagic and benthic processes is involved in this approach, and we identify the major life stage that determines the peak biomass variation. The projection of future peak biomass of *A. coerulea* in BYSs is performed based on this approach and utilizing the long-term projection results of temperature changes by 2100 using the MPI-ESM-MR model from phase 5 of the Coupled Model Intercomparison Project (CMIP5) under the RCP4.5 scenario. The results indicate that global warming can certainly lead to the increase in *A. coerulea* biomass in some degree. The steady state of the highest peak biomass will be achieved during 2075~2080, with an increase of 8.4%, 5.0%, and 11.5% in the Bohai Sea, the North Yellow Sea, and the South Yellow Sea, respectively, compared to the first steady state starting in 2020 detected by the regime shift. However, the result also shows that global warming cannot consistently lead to the increase of *A. coerulea* peak biomass. As the temperature rises to a large extent, the duration of moderate temperature ranges for strobilation and growth may be reduced, and thus resulting in the decrease of peak biomass instead.

## 1. Introduction

Global warming has altered marine ecosystems, causing consequent ecological disasters, for example jellyfish blooms. During the past two decades, jellyfish blooms have been found globally with increasing intensity and frequency of outbreaks (Brotz et al., 2012). Although both climate change and human activities contribute to the increased abundance of jellyfishes, substantial long time-series of jellyfish records have suggested that climate change is the main driver of the long-term variations of jellyfish (Lynam et al., 2011; Purcell, 2012). Therefore, more attentions and efforts should be paid on the investigation of jellyfish blooms under climate warming.

*Aurelia* sp.1, now formally classified into *Aurelia coerulea* von Lendenfeld, 1884 (Scorrano et al., 2016), known as the most common nearshore bloom species distributed worldwide (Schroth et al., 2002), is one of the most concerned species of jellyfish. Blooms of *A. coerulea* have been observed to cause negative ecological and socio-economic impacts in many areas. The Bohai and Yellow Seas (BYSs), which are important coastal seas in the western Pacific Ocean, have been suffered from *A. coerulea* blooms recently. The blooms of *A. coerulea* have created hazards that clog the cooling water intakes at coastal power plants, block fishing nets, and sting tourists over the last decades, which has

* Corresponding author.
*E-mail address:* cuicui.zhang@tju.edu.cn (C. Zhang).

https://doi.org/10.1016/j.ecolind.2023.110257
Received 11 February 2023; Received in revised form 10 April 2023; Accepted 12 April 2023
Available online 22 April 2023

been ranked as the second largest ecological disaster in BYSs (Dong et al., 2010). Moreover, the BYSs are very sensitive to climate change due to their hydrological properties of shallow, semi-enclosed, and weak water exchange capacity (Chu et al., 2005) and thus making them be more likely to be suffered from jellyfish bloom disasters. As global warming has become a serious problem, understanding the future pattern of *A. coerulea* variation in BYSs under the global warming is crucially important for ecological disaster prevention and mitigation.

As *A. coerulea* is highly adaptable to environmental changes due to its complex life history, a sufficient comprehension of the key controlling factors determining the intensity of *A. coerulea* outbreaks under climate change is a prerequisite for projection. Previous studies have shown that the life cycle of *A. coerulea* alternates between pelagic and benthic stages (Lucas, 2001), of which two critical periods affect the magnitude of blooms most. The first critical period is the benthic polyp strobilation stage, which determines the abundance of the population. The second critical period occurs during the pelagic ephyra growth, which determines the individual size of *A. coerulea* (Henschke et al., 2018). Many research efforts have been conducted to address the impacts of various environmental conditions including temperature, salinity, light conditions, pH, dissolved oxygen concentrations, and food concentrations on the polyp strobilation stage (Han and Uye, 2010; Purcell, 2005; Willcox et al., 2007; Liu et al., 2009; Ishii et al., 2008) and the ephyra growth stage (Algueró-Muñiz et al., 2016; Fu et al., 2011; Wang and Li, 2015; Widmer, 2005). They have recognized that the sea water temperature is the key environmental factor determining the intensity of blooms (Purcell, 2012; Treible and Condon, 2019; Wang and Sun, 2015; Shi et al., 2016). The influence of sea water temperature is not only reflected in the absolute value, but also in the accumulated temperature, namely the duration of moderate temperature ranges for propagation and living. In BYSs, abundant experiments show that the duration of the spring bottom temperature in the range of 10–16 °C, and the duration of the summer surface temperature in the range of 16–24 °C are the decisive factors for polyp strobilation and ephyra growth, respectively (Zhang et al., 2022; Shi et al., 2016; Fu et al., 2011). That is, the prediction of *A. coerulea* can be achieved based on the analysis of moderate temperature duration (in days) and its influences on the polyp strobilation and ephyra growth.

However, although the relationship between environmental factors and *A. coerulea* populations is well studied, its application in the projections of *A. coerulea* in BYSs remains relatively scarce. And considering the high plasticity of *A. coerulea* genus which may contribute to variable responses of *A. coerulea* to climate warming in different regions (Dawson et al., 2015), the changes of *A. coerulea* in BYSs are also difficult to infer from the studies carried out in other seas. Two limitations of current prediction methods lead to variation and uncertainty in *A. coerulea* biomass projection to some extent. Firstly, the current biomass determination method does not consider the whole life history stage thoroughly. Although previous studies have found that the different life stages of *A. coerulea* exhibit different strategies in response to sea temperature changes, the current predictions are still inferred from the analysis of each life stage isolatedly, leading to inconsistent conclusions. For example, Loveridge et al. (2021) suggests that climate warming will inhibit *A. coerulea* by analyzing the effect of temperature and its duration on polyp strobilation, while Algueró-Muñiz et al. (2016) speculates that global warming will not have a substantial impact on *A. coerulea* by examining the effects of temperature on development and survival of ephyra. Secondly, the reasonable assessment of changes in environmental conditions is still insufficient. Previous studies have shown that both temperature and the duration of moderate temperature ranges for propagation and living have a great effect on variations in *A. coerulea* populations. However, in contrast to the definitive warming trends in sea temperatures by the end of the 21$^{st}$ century, whether the duration of characteristic temperature ranges is increasing or not is still uncertain. Because of the lack of assessments of how the duration of characteristic temperature ranges varies, the temperature design of experiments differs among laboratory experiments depending on the researcher's understanding of changing sea temperature conditions. For instance, based on the same life history stage and different designs that simulate changes in winter temperature conditions, Holst (2012) indicates that climate warming is beneficial to the *A. coerulea* blooms, while Loveridge et al. (2021) suggests that climate warming is detrimental to the *A. coerulea* blooms. Therefore, the specific changes in the duration of suitable sea temperatures under climate changes and their impacts on all key life stages of *A. coerulea* should be more carefully considered during estimating future *A. coerulea* blooms.

Correlating the climate estimation result with the population model is one of the most effective ways to address these issues. The climate models represented by the Coupling Model Intercomparison Project (CMIP) are available to solve the shortcomings of existing population models of *A. coerulea* in climate simulations, while the population models enable an integrated assessment of the response of different life stages to environmental change. Since the two types of models are independent of each other, there is considerable flexibility in the choice of models when combining them. To improve the accuracy and efficiency of projection, several characteristics must be considered, including the horizontal resolution and the scenario of the climate model (Zhou et al., 2020). Phase 5 of CMIP (CMIP5) is one of the main international collaboration frameworks for physical studies in BYSs. It contains multiple models under various climate scenarios including the representative concentration pathways (RCP) 2.7, 4.5, 6.0, and 8.5. Referring to the existing climate model assessments based on the spatial distribution and interannual variability of SST, the MPI-ESM-MR model of CMIP5 under the RCP4.5 scenario is the best choice for projecting sea temperatures in BYSs. Because this model presents low errors with high resolution (Zhang et al., 2020). And RCP4.5 is a medium-mitigation emission scenario which is close to the current rate of greenhouse gas emissions. As for the population model of *A. coerulea*, the statistical relationship between the biomass and the abundance, and the effective accumulated temperature, which is simplified from the population-dynamic model by Zhang et al. (2022), is the most appropriate model for projection of *A. coerulea* biomass. Because it is accurate to reflect the linkage between temperature and the *A. coerulea* population. However, the combination of these selected models has not yet been exploited to predict the blooms of *A. coerulea* in BYSs by 2100. It's mainly because the high mobility of jellyfish challenged us to determine the appropriate habitat for benthic polyp stages.

In this study, we introduce a regional moderate-temperature-duration approach to solve this problem. This approach is updated from the simplified population model proposed in Zhang et al. (2022). The improvement is the rational zoning based on the living habits of *A. coerulea* and the dynamical nature of BYSs, which makes it possible to estimate the peak biomass of *A. coerulea* by applying corresponding regional average sea temperatures. We validate this approach with historical *A. coerulea* observations in Qinhuangdao coastal area and simulations of regional *A. coerulea* peak biomass in the Bohai Sea. Then we project the future peak biomass of *A. coerulea* in BYSs based on the regional moderate-temperature-duration approach. To reveal the specific variation of *A. coerulea* peak biomass, we conduct projections in both spatial and temporal ways. Spatially, we divide BYSs into three representative regional parts: the Bohai Sea (BS), the North Yellow Sea (NYS), and the South Yellow Sea (SYS), according to their hydrological characteristics. And then we analyze the peak biomass variations in these three areas, respectively. Temporally, we analyze the decadal peak biomass variations centered in the years of 2040, 2060, 2080, and 2100 compared to those in 2020. We also investigate the transitions of the mean level of time series fluctuations between steady-state periods, which are detected by the sequential regime shift detection method. Furthermore, to better understand the mechanisms that lead to changes in peak biomass, the major life stage that determines the peak biomass variation is analyzed.

The remainder of this article is as follows: Section 2 introduces the

data, basic material, the strategy for bottom temperature determination, and statistical analysis method used for biomass estimation and variation analysis; Section 3 presents the regional moderate-temperature-duration approach applied in long-term jellyfish biomass projection; Section 4 shows the results, including the validation of the approach, the estimate and analysis of *A. coerulea* biomass in representative time periods (2020, 2040, 2060, 2080, and 2100) and in the steady-state periods; Section 5 concludes this paper.

## 2. Material and data

### 2.1. Study area

The study area, as shown in Fig. 1, comprises of the Bohai Sea, the North Yellow Sea, and the South Yellow Sea. The Bohai Sea is a shallow sea basin surrounded by land on three sides, with an average water depth of 18 m and a coastal water depth of less than 10 m. It is characterized by the strong closure, weak water exchange capacity, obvious seasonal variation of sea temperatures, and being extremely susceptible to climate influences (Su, 1998; Jia et al., 2018; Lin et al., 2001). The Yellow Sea is a semi-enclosed shallow sea that can be divided into the North and South Yellow Seas, with an average water depth of 44 m (Su, 1998), making the sea temperatures sensitive to climate variations (Chu et al., 2005). Such shallow and semi-closed sea areas are suitable environments for the *A. coerulea* blooms.

### 2.2. Prio-knowledge on the relationship between temperature and *A. coerulea* biomass

The statistical relationships between *A. coerulea* populations and temperatures proposed in Zhang et al. (2022) were used to estimate the *A. coerulea* peak biomass. These relationships involve two key life stages of *A. coerulea*: the polyp strobilation stage, in which ephyrae are released from offshore sea bottoms; and the ephyrae growth stage, in which ephyrae grow into medusa at sea surfaces far from shore. The former stage determines the abundance while the latter determines individual weight. The combination of abundance and the individual weight contribute to the peak biomass. The influence of temperature on these two stages can be reflected by the effective durations of accumulated temperature: presented as the days of suitable temperature ranges in (10–16 °C) for strobilation in the first stage and that ranges in (16–24 °C) for individual growth in the second stage. The abundance $N$ and the average individual dry weight $IW$ at the peak time of biomass can be determined by the duration days (Zhang et al., 2022) as follows:

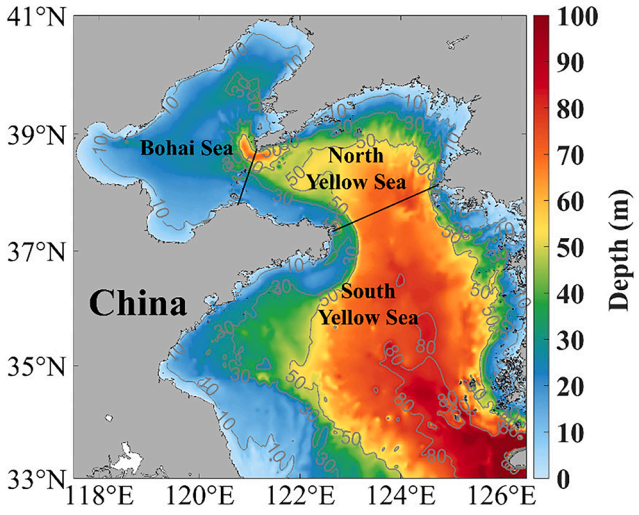


**Fig. 1.** Water depth map in the Bohai and Yellow Seas.

$$N = 0.94 \times 10^6 x_b + 1.10 \times 10^6, \quad (1)$$

$$IW = -0.322 x_s^2 + 42.21 x_s + 47.69, \quad (2)$$

where $x_b$ is the duration of 10–16 °C of sea bottom temperature in strobilation areas, and $x_s$ is the duration of 16–24 °C of sea surface temperature in growth area. Thereafter, the peak biomass $S$ can be determined by the following equation:

$$S = N \times IW. \quad (3)$$

### 2.3. Data

In this study, we selected daily sea surface temperature (SST) data from 2006 to 2100 under the RCP4.5 scenario of the Max Planck Institute Earth System Model of medium resolution (MPI-ESM-MR) model from CMIP5 for the future analysis of *A. coerulea* peak biomass variations. We used the 1993∼2019 Global Ocean Reanalysis and Simulation Project (GLORYS12V1) daily SST and sea bottom temperature (SBT) data from Copernicus Monitoring Environment Marine Service (CMEMS) for the historical analysis as well as for model validation. We used the monthly World Ocean Atlas 2018 (WOA18) data from the National Oceanic & Atmospheric Administration (NOAA) for the verification of the MPI-ESM-MR model validity. The introduction of these data are illustrated in Table 1.

For the future estimation, we used the daily SST data of the MPI-ESM-MR model because among all representative CMIP5 models suitable for the study area, the MPI-ESM-MR model has the highest resolution and its simulation result is most similar to observations (Zhang et al., 2020). In this study, we utilized the SST data instead of SBT data since the data we used require daily time resolution according to the equations mentioned in Section 2.2. However, all CMIP5 models provide only daily SST data without daily SBT data. Since SBT data are only required in offshore sea bottom where the water column is well mixed without stratification, we use daily SST data for both benthic and pelagic stages thanking to its shallow depth.

The GLORYS12V1 product from 1993 to 2019 was used for approach validation because of the following advantages: (1) the GLORYS12V1 provides very high resolution in both spatial and temporal fields with a horizontal resolution of 0.083° and the time resolution of daily and it covers a long and continuous simulation, sufficient to calculate the duration of suitable SST and SBT in BYSs; (2) the quality of GLORYS12V1 data is guaranteed since it assimilates a large number of observations (Drévillon et al., 2022a), and it provides a correction for the slowly evolving large-scale biases in temperature and salinity by a three-dimensional variational (3D-VAR) scheme (Buongiorno Nardelli, 2020; Drévillon et al., 2022b).

The WOA18 data from 2005 to 2017 was used for CMIP5 validity verification by comparing it with the simulation results at the current stage (the average over 2006 to 2017) (Lu et al., 2021). WOA data provides global analyzed observation data of *in situ* temperature at standard depth levels and its monthly results are multi-year averages over 2005 to 2017 (Locarnini et al., 2018).

To make the simulation result of MPI-ESM-MR more smoothly, we performed a multi-year average for the simulation results on all years from 2006 to 2100. The final results for 2020, 2040, 2060, 2080, and 2100 are obtained from the average over 2016∼2024, 2036∼2044, 2056∼2064, 2076∼2084, and 2096∼2100, respectively.

### 2.4. Bottom temperature determination strategy

Understanding the spatial and temporal variability of surface and bottom temperatures in BYSs provides a better understanding of biomass variation. However, neither the WOA18 data nor the CMIP5 data directly supply the bottom temperature parameter. Instead, they provide

**Table 1**
Introduction of the data used in this paper.

| Data | Variables | Time period | Temporal resolution | Spatial resolution | Reference |
|---|---|---|---|---|---|
| GLORYS12V1 | SST,SBT | 1993∼2019 | Daily | 0.083°*0.083° | (Drévillon et al., 2022a) |
| WOA18 | SST | 2005∼2017 | Monthly | 0.25°*0.25° | (Locarnini et al., 2018) |
| MPI-ESM-MR | SST | 2006∼2100 | Daily | 0.1°*0.1° | (Jungclaus et al., 2013) |

the potential temperature simulation results. Based on the potential temperature and the depth map of the study area, we therefore proposed a bottom temperature determination strategy. The bottom temperature of each grid point can be calculated by assigning it the water temperature at the depth of the bottom. The details are as follows: for the depth (d) of each grid point, we first establish its vertical layer (k), where d is higher than the depth at layer k and lower than or equal to the depth of layer k + 1. Then, we assign the water temperature of layer k as the bottom temperature to this grid point. Finally, we can get the bottom temperature map covering all the grid points.

### 2.5. *Sequential regime shift detection method*

The sequential regime shift detection method (Rodionov, 2006) was used to explore the transition between steady-state periods of peak biomass change in *A. coerulea*. In this approach, the criterion for a transition is that the difference between the mean values of both the previous and the current regimes being longer than the length of the cut-off is at least statistically significant at a given level. This means that the null hypothesis that the mean values of the two regimes are equal at this level of significance is rejected by a two-tailed Student t-test (Rodionov, 2006). Given the persistent fluctuations in the dataset, we used cut-off length of 10 years for the future analysis (2006∼2100) test at a given significance level of 0.1. The procedure is available from Bering Climate: https://www.beringclimate.noaa.gov/regimes/.

## 3. Regional moderate-temperature-duration approach for peak biomass determination

Although the determination of peak biomass based on temperature-dependent duration defined in Eqs. (1)–(3) allows for a theoretical assessment of peak biomass, it is still very difficult to calculate the quantitative peak biomass due to the high mobility of jellyfishes during benthic polyp stages (Rekstad et al., 2021). Therefore, we introduced a regional moderate-temperature-duration approach based on the region-average strategy to solve this problem.

The essential idea behind the region-average strategy is to divide the whole BYSs area into several representative zones and to determine the peak biomass of a certain region by using the regional abundance and regional average individual dry weight. Two key aspects need to be considered in the zoning division. The first is the habitats of *A. coerulea* at different life history stages to obtain environmental conditions that match the life history stages as closely as possible. Second, the divided zones need to cover representative hydrographic characteristics that can reflect both similarities within the region and differences outside to rationalize the results of temperature averaging. For the description of habitats, the polyps mainly settled on the substrates in shallow offshore waters while the ephyrae usually registered inshore and then extended to the central area (Sun et al., 2019). Thus, we preliminarily divided the entire sea area into strobilation and growth zones. The former is manifested as coastal bottom areas at water depths of less than 10 m, while the latter is the entire region. Subsequently, they are described as the source region and aggregation region, respectively. For the second consideration, the whole region is divided into hydrological zones according to the spatial distribution of projected temperature changes and existing hydrological perceptions about the water exchange capacity between the Bohai Sea and the Yellow Sea and the characteristics of water masses within the Yellow Sea. As shown in Fig. 2, the average

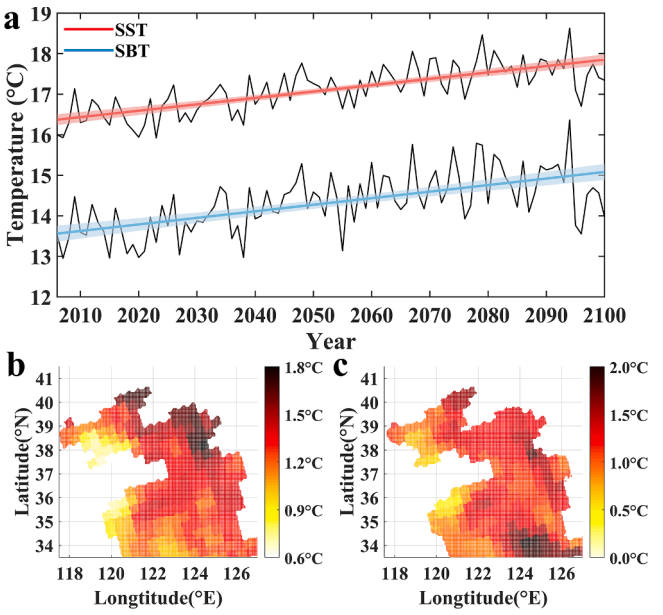


**Fig. 2.** Projected changes of water temperature in the Bohai and Yellow Seas by the end of the 21st century: (a) the annual mean surface and bottom temperature of the Bohai and Yellow Seas from 2006∼2100; (b) the difference of annual mean surface temperature between 2090 and 2010; (c) the difference of annual mean bottom temperature between 2090 and 2010. The projections are assessed by the MPI-ESM-MR model under a medium emission scenario (RCP4.5).

increases of SST and SBT in BYSs can be nearly 1.5 °C until 2090, and the highest increase of SST and SBT are obtained in the North Yellow Sea and the South Yellow Sea, which are 1.8 °C and 2.0 °C, respectively. In addition, a more consistent variability within the three sub-regions can be found in Fig. 2 (b)(c), while the water exchange capacity between the Bohai Sea and the North Yellow Sea is currently known to be weak (Su, 1998), and the North and South Yellow Seas are also relatively independent to each other due to the Yellow Sea Cold Water Mass (Xin et al., 2015). Such hydrological characteristics contribute to the habits and dynamics of *A. coerulea* being homogeneous within each region and heterogeneous between regions. Considering all the above-mentioned aspects, we divided the whole source and aggregation regions into three representative subregions: the Bohai Sea, the North Yellow Sea, and the South Yellow Sea, respectively.

The final regional division results of the source and aggregation regions are shown in Fig. 3 (a) and (b), respectively. This division is based on the assumption that the abundance of *A. coerulea* in each sea area is supplemented by its corresponding source region completely. That is, *A. coerulea* from each sea area is reproduced in the corresponding source region of each sea area and grows up in the corresponding aggregation region of each sea area. Furthermore, we assume that the abundance and individual size of *A. coerulea* in each sea area are determined by the duration (in days) of the average sea bottom temperature of 10–16 °C in the related source region and the duration (in days) of the average sea surface temperature of 16–24 °C in the relevant aggregation region, respectively. Our approach introduces the region-average strategy to the *A. coerulea* population model that depends on the duration of suitable

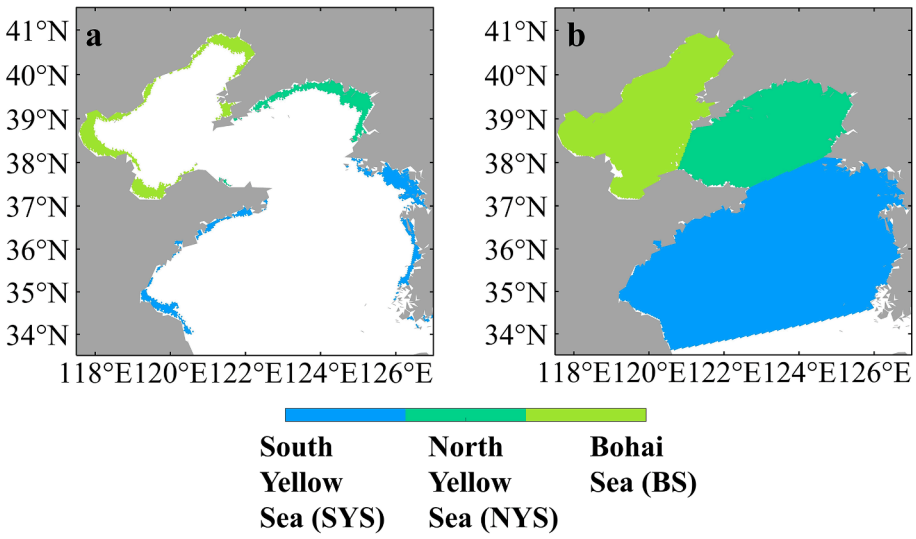


**Fig. 3.** Division of the (a) source region and (b) aggregation region.

temperature ranges. We give this approach a name as regional moderate-temperature-duration approach. By using this region-average approach, quantitative estimation and projection become possible.

## 4. Projection results and discussion

### 4.1. Validation of the regional moderate-temperature-duration approach

Although the validation of the temperature-duration-dependent *A. coerulea* model has been carried out by Zhang et al. (2022), we need to investigate more comprehensively the effectiveness of this statistical regional moderate-temperature-duration approach by comparing the historical jellyfish biomass estimation with the actual observations. As this model is a regional model for *A. coerulea* in BYSs, it may not be applicable to other seas. And among the three subregions mentioned above, the BS has relatively more *A. coerulea* records. Thus, we used this area to validate the regional moderate-temperature-duration approach.

We first calculate the peak biomass by using the determined abundance and the average individual dry weight based on the regional temperature-related duration approach. Then we compare the simulated trends with those obtained from observations. The simulation results are shown in Fig. 4. We can see that the peak biomass of *A. coerulea* in the BS significantly decreased from 2008 to 2010, then increased from 2010 to 2014, and from 2014 to 2018, it decreased again. These trends generally accord with the observations of the *A. coerulea* population in Yuan et al. (2021), which suggested that during 2008∼2015, the abundance of *A. coerulea* near Qinhuangdao in the BS decreased from 2008 to 2011, increased from 2011 to 2013, and decreased again from 2013 to 2015. In addition, our simulation results show an high abundance in 2008, which is consistent with the observation results in Yuan et al. (2021). This further demonstrates the effectiveness of our method.

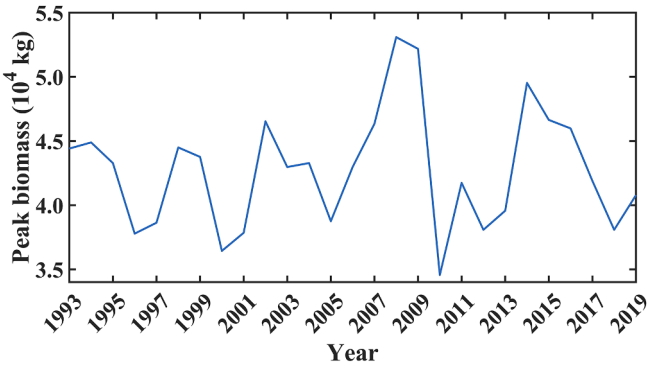


**Fig. 4.** The assessments of annual peak biomass in the Bohai Sea, 1993∼2019.

### 4.2. Decadal projection and analysis of A. coerulea peak biomass by 2100

In this experiment, we study the decadal *A. coerulea* biomass changes in representative periods (2020, 2040, 2060, 2080, 2100) using MPI-ESM-MR SST daily data. The results are illustrated in Table 2 and Fig. 5, respectively, which show the variations in temperature-related duration days, average individual dry weight, abundance, and peak biomass, respectively. From Table 2 and Fig. 5, we can see that for all the aforementioned representative periods, the SYS has the highest peak biomass among all sea areas, followed by the NYS and the BS. Besides the spatial variation, we also study the temporal changes of *A. coerulea* peak biomass in each sea area. From Table 2, we can see that compared with the peak biomass in 2020, the remarkable peak biomass rises are obtained in 2080, with a remarkable increase of 0.49 ($10^4$ kg) in the BS and the SYS. Considering the peak biomass variation between 2040 and 2020, 2060 and 2040, 2080 and 2060, 2100 and 2080, we can see that the highest increase in all sea areas is obtained in the NYS from 2060 to 2080 with an increase of 0.45 ($10^4$ kg), followed by that in the BS from 2060 to 2080 with an increase of 0.43 ($10^4$ kg). By comparing the trend changes of abundance, average individual dry weight, and peak biomass in Fig. 5 (c)–(e), we find that the variation of abundance is generally similar to the trend of peak biomass, which presents the same spatial characteristics. Thus, we believe that the abundance of jellyfish is the key factor in determining the peak biomass, and the average individual dry weight of jellyfish plays a less important role.

Since the abundance is determined by the duration of suitable temperature ranges for strobilation (10–16 °C), we analyze the specific differences in the duration (in days) of each sea area in 2040, 2060, 2080, and 2100, respectively. From Fig. 5 (a), and Table 2, we can see that both in the BS and the SYS, the strobilation-related durations show a trend of increasing duration from 2020 to 2080 and decreasing duration from 2080 to 2100. However, in the NYS the duration shows a decreasing trend from 2020 to 2060, an increasing trend from 2060 to 2080, and then followed by a decreasing trend again from 2080 to 2100. In particular, strobilation-related duration increases by 5 days from 2020 to 2080 and decreases by 4 days from 2080 to 2100 in both the BS

**Table 2**
Future estimation of temperature-related duration, abundance, and average individual dry weight (IW) in the Bohai and Yellow Seas in representative time periods.

| Variables | Area | 2020 | 2040 | 2060 | 2080 | 2100 | 2040-2020 | 2060-2020 | 2080-2020 | 2100-2020 | 2060-2040 | 2080-2060 | 2100-2080 |
|---|---|---|---|---|---|---|---|---|---|---|---|---|---|
| Duration days of suitable strobilation SST (day) | Bohai Sea | 30 | 30 | 31 | 35 | 31 | 0 | 1 | 5 | 1 | 1 | 4 | −4 |
| | North Yellow Sea | 36 | 35 | 32 | 35 | 31 | −1 | −4 | −1 | −5 | −3 | 3 | −4 |
| | South Yellow Sea | 38 | 39 | 42 | 43 | 39 | 1 | 4 | 5 | 1 | 3 | 1 | −4 |
| Duration days of suitable growth SST (day) | Bohai Sea | 56 | 52 | 53 | 50 | 56 | −4 | −3 | −6 | 0 | 1 | −3 | 6 |
| | North Yellow Sea | 61 | 55 | 58 | 62 | 58 | −6 | −3 | 1 | −3 | 3 | 4 | −4 |
| | South Yellow Sea | 58 | 58 | 54 | 52 | 58 | 0 | −4 | −6 | 0 | −4 | −2 | 6 |
| Abundance ($10^7$ ind) | Bohai Sea | 2.93 | 2.93 | 3.02 | 3.40 | 3.02 | 0.00 | 0.09 | 0.47 | 0.09 | 0.09 | 0.38 | −0.38 |
| | North Yellow Sea | 3.49 | 3.40 | 3.12 | 3.40 | 3.02 | −0.09 | −0.38 | −0.09 | −0.47 | −0.28 | 0.28 | −0.38 |
| | South Yellow Sea | 3.68 | 3.78 | 4.06 | 4.15 | 3.78 | 0.09 | 0.38 | 0.47 | 0.09 | 0.28 | 0.09 | −0.38 |
| IW ($10^3$ mg) | Bohai Sea | 1.40 | 1.37 | 1.38 | 1.35 | 1.40 | −0.03 | −0.02 | −0.05 | 0.00 | 0.01 | −0.03 | 0.05 |
| | North Yellow Sea | 1.42 | 1.40 | 1.41 | 1.43 | 1.41 | −0.03 | −0.01 | 0.00 | −0.01 | 0.02 | 0.01 | −0.01 |
| | South Yellow Sea | 1.41 | 1.41 | 1.39 | 1.37 | 1.41 | 0.00 | −0.02 | −0.04 | 0.00 | −0.02 | −0.02 | 0.04 |
| Peak biomass ($10^4$ kg) | Bohai Sea | 4.11 | 4.02 | 4.17 | 4.60 | 4.24 | −0.09 | 0.07 | 0.49 | 0.13 | 0.15 | 0.43 | −0.36 |
| | North Yellow Sea | 4.98 | 4.74 | 4.40 | 4.85 | 4.27 | −0.23 | −0.57 | −0.13 | −0.70 | −0.34 | 0.45 | −0.58 |
| | South Yellow Sea | 5.20 | 5.33 | 5.63 | 5.70 | 5.33 | 0.13 | 0.43 | 0.49 | 0.13 | 0.30 | 0.06 | −0.36 |

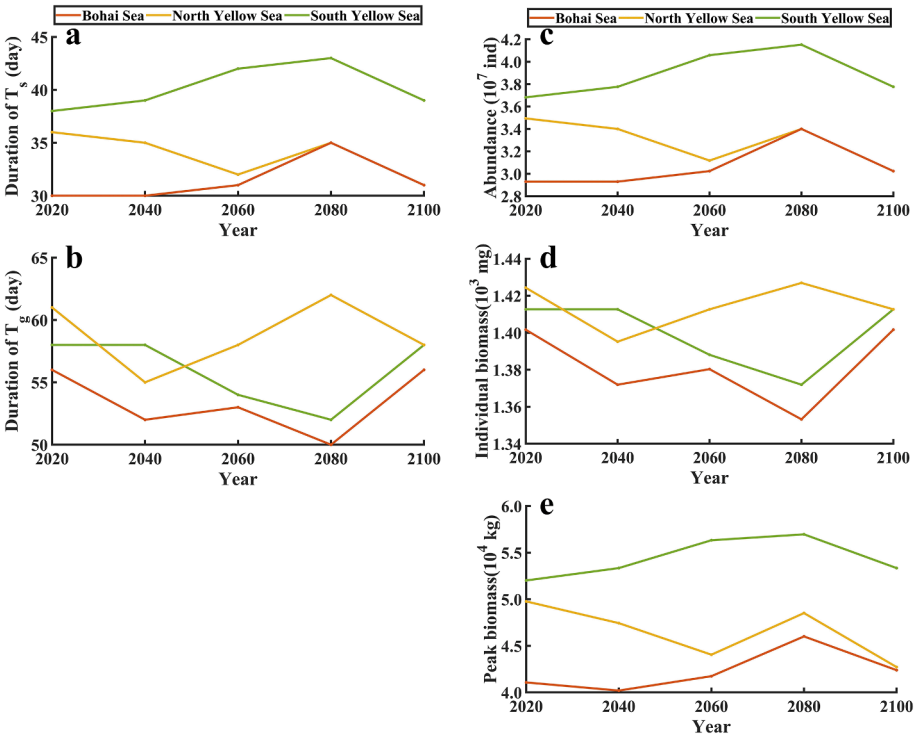


**Fig. 5.** Future decadal projection of (a) duration for strobilation (in days), (b) duration for growth (in days), (c) abundance, (d) average individual dry weight and (e) peak biomass in the Bohai and Yellow Seas in representative time periods (2020, 2040, 2060, 2080, 2100).

and the SYS; in the NYS, it decreases by 4 days from 2020 to 2060, increases by 3 days from 2060 to 2080, and decreases by 4 days from 2080 to 2100. For a better understanding of the *A. coerulea* phenology, we investigate the daily variations of average SST in the source regions of the BS, the NYS, and the SYS in representative periods (see Fig. 6 (a)–(c)). Combining Fig. 6 with the findings obtained from Table 2 and Fig. 5, we can see that the SYS has the longest duration due to its early start time. Comparing SYS to BS, we can see that they have a similar end time, but SYS has an earlier start time. Comparing SYS to NYS, SYS shows an earlier start time and end time than NYS, and SYS has a greater advance in the start time. Besides, the NYS has a longer duration than BS in 2020, 2040, and 2060, while in 2080 and 2100 the durations in the NYS and the BS are almost the same. These changes can be mainly characterized by the postponed start and end times in the NYS and a great delay in the end time in 2020, 2040, and 2060. Based on these findings, it can be concluded that the duration in the SYS and the BS is determined by the start time, that is, the point in time when the sea temperature reaches 10 °C. And in the NYS, the duration is determined by the end time, which is the point in time when the sea temperature reaches 16 °C. Furthermore, focusing on the temporal variation of duration, we can see that, in all sea areas, the start and end times of the strobilation-related duration are earlier in 2100 than those in 2020,

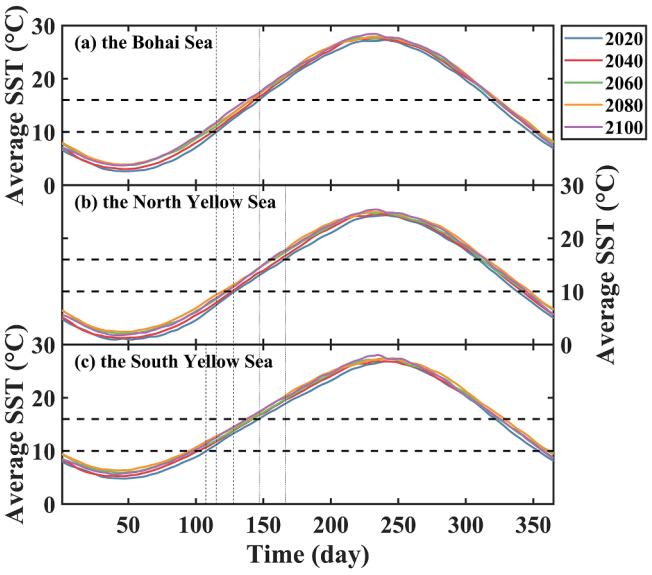


**Fig. 6.** Daily variations of average SST in the source regions of (a) the Bohai Sea, (b) the North Yellow Sea, and (c) the South Yellow Sea during representative periods (2020, 2040, 2060, 2080, 2100).

which suggests a possible advance in the phenology of *A. coerulea*.

### 4.3. *Estimation of A. coerulea peak biomass in steady-state periods*

In this section, we investigate the transition between steady-state periods of *A. coerulea* peak biomass based on shift detection. The transition between steady-state periods are detected from a long-term yearly estimated sequence, which are obtained based on the calculation approach mentioned in Section 3. The results are shown in Table 3 and Fig. 7, respectively. We can see that the steady-state variations of *A. coerulea* peak biomass in the BS exhibit periodic changes with an average period of about 10 years (6∼16 years), and most steady-state

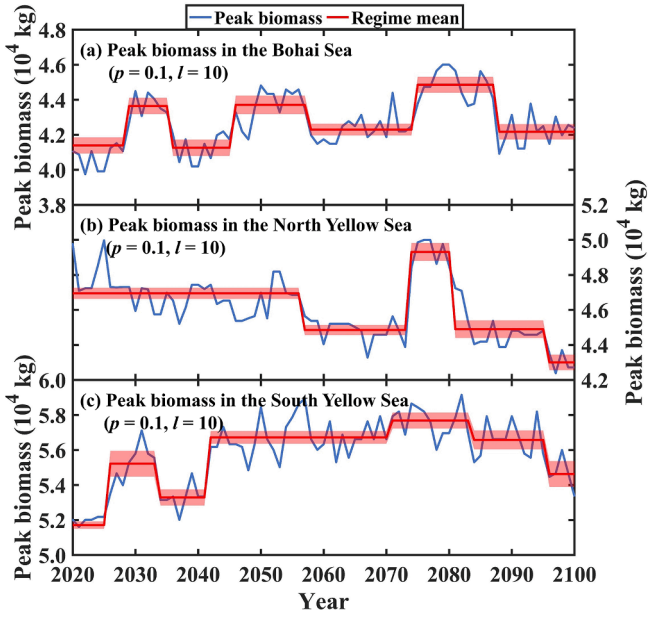


**Fig. 7.** Estimations of annual peak biomass in (a) the Bohai Sea, (b) the North Yellow Sea, and (c) the South Yellow Sea, 2020∼2100 (blue lines). The red lines show regime shifts in the mean level of fluctuations of peak biomass, the cut-off length of 10 years, and the maximum significance level of $p = 0.1$. The red shadows indicate the 95% confidence intervals of the regime mean.

changes are significant by more than 5% rate of change (ROC). In the NYS, the current steady state lasts about 35 years, after which steady state shifts occur every about 15 years, and the strongest shift for the whole period is in 2073∼2074 with a rate of change of 9.80%. In the SYS, seven shift points are detected, which are characterized by two transitions from low to high and back to low steady state until 2042, with the largest increase around 2025 and maintaining a high steady state for nearly 50 years after 2042. Through comparing steady-state variations in these sea areas, we find that they share a similar trend as follows: there is a very high peak biomass steady state from 2075 to 2080 and a relatively low peak biomass steady state over the period 2096∼2100. During the high peak biomass steady state, the peak biomass in the BS, the NYS, and the SYS increased at a maximum rate of 8.4%, 5.0%, and 11.5%, respectively, compared to the first steady state starting in 2020, as shown in Table 3. From these findings, we can draw that global warming can indeed lead to an increase in jellyfish biomass to a certain extent. However, this influence is not the continuous when the temperature is increased to a large extent since such a high temperature may even not be suitable for the propagation and growth of jellyfish.

Next, we perform more experiments to further investigate which is the key factor that determines the peak biomass: the abundance or the average individual dry weight. In Section 4.2, we qualitatively drew that the abundance is the determinant by comparing the trend changes. Here we want to quantitatively investigate the key factor through statistical analysis of the estimated time series of interannual peak biomass. Table 4 demonstrates the coefficient of determination and correlation between peak biomass and abundance, and that between peak biomass and individual biomass, as well as the coefficient of variation for abundance and that for individual biomass. The meaning and calculation of these coefficients are shown in the footnotes of Table 4. From Table 4, we can see that the coefficient of determination between abundance and peak biomass is above 0.73 in all sea areas, with the contribution of abundance to peak biomass even reaching 94% in the SYS, while the coefficient of determination between average individual dry weight and peak biomass is at most 0.12. Besides, the coefficient of correlation between abundance and peak biomass is much greater than that between average individual dry weight and peak biomass, reaching a maximum of 0.97. Also, the coefficient of variation in abundance is higher than that in average individual dry weight. These results suggest that abundance accounts for the majority of the variation in peak biomass. And because the life stage that determines abundance is the benthic polyp strobilation stage, we can further confirm that the benthic polyp strobilation stage is the key life stage determines the variability of *A. coerulea* peak biomass.

## 5. Conclusion and future work

This paper investigated the long-term *A. coerulea* biomass changes in BYSs by 2100 using the CMIP5 model data under RCP4.5. The projection of *A. coerulea* biomass in interdecadal representative periods (2020, 2040, 2060, 2080, 2100) and the steady-state periods from interannual time series were performed based on the statistical relationships between the *A. coerulea* biomass and sea temperatures. The former results indicate that in BYSs, there will be an earlier timing of *A. coerulea* phenology compared to the current situation. The variations analyzed from the transition between steady-state periods suggest that we should pay more attention to the period from 2075 to 2080 when all sea areas in BYSs exhibit high peak biomass steady state. Apart from this, the three sea areas show differences in the salient characteristics of steady-state variability at other times. In the BS, the most significant characteristic of steady-state variability is that it exhibits cyclical changes with an average period of 10 years. In the NYS, the most notable change is the rapid increase in 2073∼2074. In the SYS, the outstanding feature regarding the steady state is the high steady state that persists for almost 50 years after 2042. However, the low peak biomass steady state over

**Table 3**
Future estimation of peak biomass ($10^4$ kg) in the Bohai and Yellow Seas in steady-state periods.

| Area | 2020∼2028 | 2029∼2035 | 2036∼2045 | 2046∼2057 | 2058∼2074 | 2075∼2087 | 2088∼2100 | ROC1 | ROC2 | ROC3 | ROC4 | ROC5 | ROC6 |
|---|---|---|---|---|---|---|---|---|---|---|---|---|---|
| Bohai Sea | 4.14 | 4.36 | 4.13 | 4.37 | 4.23 | 4.49 | 4.22 | 5.31% | −5.28% | 5.81% | −3.20% | 6.15% | −6.01% |
| **Area** | **2020∼2056** | **2057∼2073** | **2074∼2080** | **2081∼2095** | **2096∼2100** | **ROC1** | **ROC2** | **ROC3** | **ROC4** | | | / | |
| North Yellow Sea | 4.69 | 4.49 | 4.93 | 4.49 | 4.30 | −4.26% | 9.80% | −8.92% | −4.23% | | | / | |
| **Area** | **2020∼2025** | **2026∼2033** | **2034∼2041** | **2042∼2070** | **2071∼2083** | **2084∼2095** | **2096∼2100** | **ROC1** | **ROC2** | **ROC3** | **ROC4** | **ROC5** | **ROC6** |
| South Yellow Sea | 5.17 | 5.52 | 5.33 | 5.67 | 5.77 | 5.66 | 5.46 | 6.77% | −3.44% | 6.38% | 1.76% | −1.91% | −3.53% |

**Table 4**
Coefficient of determination, correlation, and variation between abundance (Abu.), average individual dry weight (IW), and peak biomass.

| Area | Determination[1] | | Correlation[2] | | Variation[3] | |
|---|---|---|---|---|---|---|
| | Abu. | IW | Abu. | IW | Abu. | IW |
| Bohai Sea | 0.73 | −0.08 | 0.87 | 0.18 | 0.06 | 0.03 |
| North Yellow Sea | 0.80 | 0.12 | 0.90 | 0.36 | 0.07 | 0.03 |
| South Yellow Sea | 0.94 | 0.12 | 0.97 | 0.37 | 0.08 | 0.02 |

[1] The coefficient of determination ($R^2$) is to measure the extent to which the independent variable explains the dependent variable. It usefully takes a value in the range 0 to 1, with greater values indicating greater relationship between the predictor and dependent variables. A negative $R^2$ indicates that the regression function is a poorer fit than taking the mean. It is calculated as follows: $R^2 = 1 - \frac{\sum \left(y_i - y_{\text{Regression}}\right)^2}{\sum \left(y_i - \overline{y}\right)^2}$, where $y_{\text{Regression}}$ is peak biomass, $y_i$ is the data points of abundance or average individual dry weight, $\overline{y}$ is the mean of abundance or mean individual dry weight.

[2] The coefficient of correlation (r) is to show the significance of the association between the two variables. It ranges from −1 to 0 to + 1, with larger absolute values indicating a more linear relationship. It is calculated as follows: $r = \frac{\sum_{i=1}^{n}(X_i - \overline{X})(Y_i - \overline{Y})}{\sqrt{\sum_{i=1}^{n}(X_i - \overline{X})^2}\sqrt{\sum_{i=1}^{n}(Y_i - \overline{Y})^2}}$, where Y is peak biomass, X is abundance or average individual dry weight.

[3] The coefficient of variation (COV) is to compare the data dispersion between distinct series of data, with larger values reflecting a greater ability of the independent variable to explain variation in the dependent variable. It is calculated as follows: $COV = \frac{\sigma}{\mu}$, where $\sigma$ is the standard deviation of abundance or average individual dry weight, $\mu$ is the mean of abundance or average individual dry weight.

the period 2096∼2100 shows that global warming cannot continuously promote jellyfish blooms. In this work, we also found that the key life stage influences the peak biomass is the benthic polyp strobilation stage, which determines the abundance of *A. coerulea*.

Due to the complexity of marine ecosystems and the continuous climate changes, the projection of the peak biomass of *A. coerulea* may have some limitations. The findings of this paper are based on the assumptions that the projection of seawater temperature is accurate and that the food concentrations (zooplankton) are adequate in the next 80 years in BYSs. However, we cannot guarantee that the simulation results of the CMIP5 models can completely meet the changes in climate in the future. Thus, for one thing, it may cause inaccuracies in the projection of the peak biomass of *A. coerulea*. For another, the biomass of zooplankton may also be affected by global warming, which may cause other uncertainties in the projection results. The potential effects of zooplankton responses to global warming have been investigated in existing works. They found that a warming climate may cause the universal responses of declines in body size (Brandão et al., 2021), poleward and/or deeper layer shifts (Ratnarajah et al., 2023), and the earlier timing of phenology (Cooley et al., 2022). However, whether these changes will result in insufficient food concentrations for *A. coerulea* in the future is still unknown. According to the existing studies, copepods, which are generally recognized as the main food source of *A. coerulea*, would increase in biomass and abundance in shallow eutrophic lakes (Cremona et al., 2020) and would exhibit higher thermal tolerance with the increase in the maximum annual temperature (Sasaki and Dam, 2021). We expect that future changes in zooplankton can generally satisfy our hypothesis that the food concentrations for *A. coerulea* are sufficient, and thus they will have little effect on the projection of *A. coerulea* peak biomass. In the future, we will investigate more specifically on the potential effect of zooplankton to the warming climate. We believe this would help us understand the potential impacts of ocean warming on the *A. coerulea* population more comprehensively.

## Formatting of funding sources

This research was funded by the National Key Research and Development Program of China (2022YFC3104600), the Municipal Nature Science Foundation of Tianjin (21JCQNJC00650), and the National Natural Science Foundation of China (41806116).

## CRediT authorship contribution statement

**Yifan Lan:** Software, Validation, Formal analysis, Investigation, Data curation, Writing - original draft, Visualization. **Cuicui Zhang:** Conceptualization, Resources, Writing - review & editing, Supervision, Project administration, Funding acquisition. **Hao Wei:** Conceptualization, Methodology, Formal analysis, Writing - review & editing.

## Declaration of Competing Interest

The authors declare that they have no known competing financial interests or personal relationships that could have appeared to influence the work reported in this paper.

## Data availability

Data will be made available on request.

## Acknowledgements

We express thanks to the editor and reviewers for their valuable comments and suggestions. This study has been conducted using the data from E.U. Copernicus Marine Service Information, WOA series products, and CMIP5 simulations. GLORYS12V1 data are available from

Copernicus Marine Environment Monitoring Service at: https://resources.marine.copernicus.eu/?option=com_csw&view=details&product_id=GLOBAL_REANALYSIS_PHY_001_030. The WOA2018 data were provided by the National Oceanographic Data Center (NODC) on the web ( https://www.nodc.noaa.gov/cgi-bin/OC5/woa18/woa18.pl). And CMIP5 data were produced by World Climate Research Programme's Working Group on Coupled Modelling and the climate modelling groups on the web ( https://esgf-node.llnl.gov/search/cmip5/).

## References


Algueró-Muñiz, M., Meunier, C.L., Holst, S., Alvarez-Fernandez, S., Boersma, M., 2016. Withstanding multiple stressors: ephyrae of the moon jellyfish (*Aurelia aurita*, Scyphozoa) in a high-temperature, high-$CO_2$ and low-oxygen environment. Mar. Biol. 163 (9), 185. https://doi.org/10.1007/s00227-016-2958-z.

Brotz, L., Cheung, W.W.L., Kleisner, K., Pakhomov, E., Pauly, D., 2012. Increasing jellyfish populations: trends in Large Marine Ecosystems. Hydrobiologia 690 (1), 3–20. https://doi.org/10.1007/s10750-012-1039-7.

Buongiorno Nardelli, B., 2020. A multi-year time series of observation-based 3D horizontal and vertical quasi-geostrophic global ocean currents. Earth Syst. Sci. Data 12 (3), 1711–1723. https://doi.org/10.5194/essd-12-1711-2020.

Chu, P., Yuchun, C., Kuninaka, A., 2005. Seasonal variability of the Yellow Sea/East China Sea surface fluxes and thermohaline structure. Adv. Atmos. Sci. 22 (1), 1–20. https://doi.org/10.1007/bf02930865.

Cremona, F., Agasild, H., Haberman, J., Zingel, P., Nõges, P., Nõges, T., Laas, A., 2020. How warming and other stressors affect zooplankton abundance, biomass and community composition in shallow eutrophic lakes. Clim. Change 159 (4), 565–580. https://doi.org/10.1007/s10584-020-02698-2.

Dawson, M.N., Cieciel, K., Decker, M.B., Hays, G.C., Lucas, C.H., Pitt, K.A., 2015. Population-level perspectives on global change: genetic and demographic analyses indicate various scales, timing, and causes of scyphozoan jellyfish blooms. Biol. Invasions 17 (3), 851–867. https://doi.org/10.1007/s10530-014-0732-z.

Dong, Z., Liu, D., Keesing, J.K., 2010. Jellyfish blooms in China: Dominant species, causes and consequences. Mar. Pollut. Bull. 60 (7), 954–963. https://doi.org/10.1016/j.marpolbul.2010.04.022.

Drévillon, M., Fernandez, E., Lellouche, J.-M., 2022a. Product User Manual for the Global Ocean Physical Multi Year product, GLOBAL_MULTIYEAR_PHY_001_030. Copernicus Marine Service. https://doi.org/10.48670/moi-00021.

Cooley, S., Schoeman, D., Bopp, L., Boyd, P., Donner, S., Ghebrehiwet, D.-Y., Ito, S.-I., Kiessling, W., Martinetto, P., Ojea, E., Racault, M.-F., Rost, B., Skern-Mauritzen, M., 2022. Oceans and coastal ecosystems and their services. In: Pörtner, H.-O., Roberts, D.-C., Tignor, M., Poloczanska, E.-S., Mintenbeck, K., Alegría, A., Craig, M., Langsdorf, S., Löschke, S., Möller, V., Okem, A., Rama, B. (Eds.), Climate Change 2022: Impacts, Adaptation and Vulnerability. Contribution of Working Group II to the Sixth Assessment Report of the Intergovernmental Panel on Climate Change. Cambridge University Press, Cambridge, United Kingdom and New York, NY, USA, p. 379–550.

Drévillon, M., Lellouche, J.-M., Régnier, C., Garric, G., Bricaud, C., Hernandez, O., Bourdallé-Badie, R., 9 2022b. Quality Information Document for Global Ocean Reanalysis Products, GLOBAL-REANALYSIS-PHY-001-030. Copernicus Marine Service.

Fu, Z., Dong, J., Sun, M., Zhao, Y., 2011. Effects of water temperature and salinity on growth of ephyrae in moon jellyfish *Aurelia* sp in North Yellow Sea in China. Fish. Sci. 30 (4), 221–224 https://doi.org/10.16378/j.cnki.1003-1111.2011.04.010.

Han, C.-H., Uye, S.-I., 2010. Combined effects of food supply and temperature on asexual reproduction and somatic growth of polyps of the common jellyfish *Aurelia aurita* s.l. Plankton Benthos Res. 5 (3), 98–105. https://doi.org/10.3800/pbr.5.98.

Henschke, N., Stock, C.A., Sarmiento, J.L., 2018. Modeling population dynamics of scyphozoan jellyfish (*Aurelia* spp.) in the Gulf of Mexico. Mar. Ecol. Prog. Ser. 591, 167–183. https://doi.org/10.3354/meps12255.

Holst, S., 2012. Effects of climate warming on strobilation and ephyra production of North Sea scyphozoan jellyfish. Hydrobiologia 690 (1), 127–140. https://doi.org/10.1007/s10750-012-1043-y.

Ishii, H., Ohba, T., Kobayashi, T., 2008. Effects of low dissolved oxygen on planula settlement, polyp growth and asexual reproduction of *Aurelia aurita*. Plankton Benthos Res. 3 (Suppl.), 107–113. https://doi.org/10.3800/pbr.3.107.

Jia, H., Shen, Y., Su, M., Yu, C., 2018. Numerical simulation of hydrodynamic and water quality effects of shoreline changes in Bohai Bay. Front. Earth Sci. 12 (3), 625–639. https://doi.org/10.1007/s11707-018-0688-x.

Jungclaus, J.H., Fischer, N., Haak, H., Lohmann, K., Marotzke, J., Matei, D., Mikolajewicz, U., Notz, D., von Storch, J.S., 2013. Characteristics of the ocean simulations in the Max Planck Institute Ocean Model (MPIOM) the ocean component of the MPI-Earth system model. J. Adv. Model. Earth Syst. 5 (2), 422–446. https://doi.org/10.1002/jame.20023.

Lin, C., Su, J., Xu, B., Tang, Q., 2001. Long-term variations of temperature and salinity of the Bohai Sea and their influence on its ecosystem. Prog. Oceanogr. 49 (1), 7–19. https://doi.org/10.1016/s0079-6611(01)00013-1.

Liu, W.-C., Lo, W.-T., Purcell, J.E., Chang, H.-H., 2009. Effects of temperature and light intensity on asexual reproduction of the scyphozoan, *Aurelia aurita* (L.) in Taiwan. Hydrobiologia 616 (1), 247–258. https://doi.org/10.1007/s10750-008-9597-4.

Locarnini, R.A., Mishonov, A.V., Baranova, O.K., Boyer, T.P., Zweng, M.M., Garcia, H.E., Reagan, J.R., Seidov, D., Weathers, K., Paver, C.R., Smolyar, I., 2018. World Ocean Atlas 2018, Volume 1: Temperature. A. Mishonov Technical Ed.; NOAA Atlas NESDIS 81, 52pp.

Loveridge, A., Lucas, C.H., Pitt, K.A., 2021. Shorter, warmer winters may inhibit production of ephyrae in a population of the moon jellyfish *Aurelia aurita*. Hydrobiologia 848 (3), 739–749. https://doi.org/10.1007/s10750-020-04483-9.

Lu, H., Xie, C., Zhang, C., Zhai, J., 2021. CMIP5-based projection of decadal and seasonal sea surface temperature variations in East China Shelf Seas. J. Mar. Sci. Eng. 9 (4), 367. https://doi.org/10.3390/jmse9040367.

Lucas, C.H., 2001. Reproduction and life history strategies of the common jellyfish, *Aurelia aurita*, in relation to its ambient environment. Hydrobiologia 451 (1), 229–246. https://doi.org/10.1023/A:1011836326717.

Lynam, C.P., Lilley, M.K.S., Bastian, T., Doyle, T.K., Beggs, S.E., Hays, G.C., 2011. Have jellyfish in the Irish Sea benefited from climate change and overfishing? Global Change Biol. 17 (2), 767–782. https://doi.org/10.1111/j.1365-2486.2010.02352.x.

Purcell, J.E., 2005. Climate effects on formation of jellyfish and ctenophore blooms: a review. J. Mar. Biol. Assoc. U.K. 85 (3), 461–476. https://doi.org/10.1017/S0025315405011409.

Purcell, J.E., 2012. Jellyfish and ctenophore blooms coincide with human proliferations and environmental perturbations. Ann. Rev. Mar. Sci. 4 (1), 209–235. https://doi.org/10.1146/annurev-marine-120709-142751.

Ratnarajah, L., Abu-Alhaija, R., Atkinson, A., Batten, S., Bax, N.J., Bernard, K.S., Canonico, G., Cornils, A., Everett, J.D., Grigoratou, M., Ishak, N.H.A., Johns, D., Lombard, F., Muxagata, E., Ostle, C., Pitois, S., Richardson, A.J., Schmidt, K., Stemmann, L., Swadling, K.M., Yang, G., Yebra, L., 2023. Monitoring and modelling marine zooplankton in a changing climate. Nat. Commun. 14 (1), 564. https://doi.org/10.1038/s41467-023-36241-5.

Rekstad, M.E., Majaneva, S., Borgersen, Å.L., Aberle, N., 2021. Occurrence and habitat characteristics of *Aurelia* sp. polyps in a high-latitude fjord. Front. Mar. Sci. 8, 684634 https://doi.org/10.3389/fmars.2021.684634.

Rodionov, S.N., 2006. Use of prewhitening in climate regime shift detection. Geophys. Res. Lett. 33 (12), L12707. https://doi.org/10.1029/2006GL025904.

Sasaki, M., Dam, H.G., 2021. Global patterns in copepod thermal tolerance. J. Plankton Res. 43 (4), 598–609. https://doi.org/10.1093/plankt/fbab044.

Schroth, W., Jarms, G., Streit, B., Schierwater, B., 2002. Speciation and phylogeography in the cosmopolitan marine moon jelly, *Aurelia* sp. BMC Evol. Biol. 2 (1), 1. https://doi.org/10.1186/1471-2148-2-1.

Scorrano, S., Aglieri, G., Boero, F., Dawson, M.N., Piraino, S., 2016. Unmasking *Aurelia* species in the Mediterranean Sea: an integrative morphometric and molecular approach. Zool. J. Linn. Soc. 180 (2), 243–267. https://doi.org/10.1111/zoj.12494.

Shi, Y., Mi, T., Wang, J., Chen, L., Wang, G., Zhen, Y., Yu, Z., 2016. The effect of temperature and food supply on the asexual reproduction of moon jelly (*Aurelia* sp.1) polyps. Acta Ecol. Sin. 36 (3), 786–794. https://doi.org/10.5846/stxb201404170751.

Su, J., 1998. Circulation dynamics of the China Seas north of 18°N. The Sea 11, 483–505.

Sun, X., Wei, H., Zhang, H., Wang, Y., Zhang, G., Liu, H., 2019. Tracing giant jellyfish in coastal waters nearby Hongyanhe Power Plant. Oceanol. Limnol. Sin. 50 (6), 1281–1291 https://doi.org/10.11693/hyhz20190600104.

Treible, L.M., Condon, R.H., 2019. Temperature-driven asexual reproduction and strobilation in three scyphozoan jellyfish polyps. J. Exp. Mar. Biol. Ecol. 520, 151204 https://doi.org/10.1016/j.jembe.2019.151204.

Wang, N., Li, C., 2015. The effect of temperature and food supply on the growth and ontogeny of *Aurelia* sp.1 ephyrae. Hydrobiologia 754 (1), 157–167. https://doi.org/10.1007/s10750-014-1981-7.

Wang, Y.-T., Sun, S., 2015. Population dynamics of *Aurelia* sp.1 ephyrae and medusae in Jiaozhou Bay, China. Hydrobiologia 754 (1), 147–155. https://doi.org/10.1007/s10750-014-2021-3.

Widmer, C.L., 2005. Effects of temperature on growth of north-east Pacific moon jellyfish ephyrae, *Aurelia labiata* (Cnidaria: Scyphozoa). J. Mar. Biol. Assoc. U.K. 85 (3), 569–573. https://doi.org/10.1017/S0025315405011495.

Willcox, S., Moltschaniwskyj, N.A., Crawford, C., 2007. Asexual reproduction in scyphistomae of *Aurelia* sp.: Effects of temperature and salinity in an experimental study. J. Exp. Mar. Biol. Ecol. 353 (1), 107–114. https://doi.org/10.1016/j.jembe.2007.09.006.

Xin, M., Ma, D., Wang, B., 2015. Chemicohydrographic characteristics of the Yellow Sea Cold Water Mass. Acta Oceanol. Sin. 34 (6), 5–11. https://doi.org/10.1007/s13131-015-0681-0.

Yuan, X., Liu, Z., Xue, L., Chen, X., An, Y., 2021. Review on the occurrence regularity and current situation of jellyfish disaster in Qinhuangdao coastal area. Hebei Fish. 330 (6), 12–17. https://doi.org/10.3969/j.issn.1004-6755.2021.06.004.

Zhang, C., Wei, H., Song, G., Xie, C., 2020. IPCC-CMIP5 based projection and analysis of future sea surface temperature changes in coastal seas East of China. Oceanol. Limnol. Sin. 51 (6), 1288–1300 https://doi.org/10.11693/hyhz20191200246.

Zhang, H., Zhang, G., Lan, Y., Xiao, J., Wang, Y., Song, G., Wei, H., 2022. A modeling study on population dynamics of jellyfish *Aurelia aurita* in the Bohai and Yellow Seas. Front. Mar. Sci. 9, 842394 https://doi.org/10.3389/fmars.2022.842394.

Zhou, T., Zhang, W., Chen, X., Zhang, L., Zhou, L., Man, W., 2020. The near-term, mid-term and long-term projections of temperature and precipitation changes over the Tibetan Plateau and the sources of uncertainties. J. Meteor. Sci. 40 (5), 697–710. https://doi.org/10.3969/2020jms.0076.

Brandão, M.C., Benedetti, F., Martini, S., Soviadan, Y.D., Irisson, J.-O., Romagnan, J.-B., Elineau, A., Desnos, C., Jalabert, L., Freire, A.S., Picheral, M., Guidi, L., Gorsky, G., Bowler, C., Karp-Boss, L., Henry, N., de Vargas, C., Sullivan, M.B., Stemmann, L., Lombard, F., Tara Oceans Consortium, C., 2021. Macroscale patterns of oceanic

zooplankton composition and size structure. Sci. Rep. 11 (1), 15714, https://doi.org/10.1038/s41598-021-94615-5.